The Influence of Stacked Actuators on Source Impedance of a Piezoelectric Spinal Fusion Implant

By

Nathan C. Goetzinger

Submitted to the graduate degree program in Bioengineering and the Graduate Faculty of the University of Kansas in partial fulfillment of the requirements for the degree of Master of Science.

_____

Chairperson Dr. Elizabeth Friis

_____

Dr. Lorin Maletsky

_____

Dr. Kenneth Fischer

Date Defended: May 27, 2014

The Thesis Committee for Nathan Goetzinger

certifies that this is the approved version of the following thesis:

The Influence of Stacked Actuators on Source Impedance of a Piezoelectric Spinal Fusion Implant

_____

Chairperson Elizabeth Friis

Date approved: _____

Abstract

The failure rate for difficult-to-fuse patients undergoing spinal fusion surgeries can be as high as 29-46%. The primary adjunct treatments which currently address this problem are bone morphogenetic proteins (BMPs) and DC electrical stimulation. BMPs have had clinical problems with off-label use and ectopic bone growth. DC electrical stimulation has had much clinical success, but it requires longer procedures (compared to surgeries with only spinal fusion cages and instrumentation) and it can require revision surgeries to remove the battery pack. To overcome these problems with current adjunct therapies, a piezoelectric spinal fusion implant has been developed which produces electrical stimulation without an external battery pack.

One of the primary obstacles with creating a piezoelectric spinal fusion implant was the extremely high source impedance due to the capacitive nature of piezoelectric materials. Stacked actuators have been used with monolithic piezoelectric elements to lower source impedance, so this approach was utilized with a 3-1 composite piezoelectric material made from PZT 5A1 fibers with EPO-TEK 301 epoxy used as the matrix material. Specimens were made with 1 layer, 3 layers, 6 layers, or 9 layers and the effects of the number of layers on average maximum power and the load resistance at which average maximum power occurred (optimal load resistance) were studied. The effects of mechanical preload, mechanical load frequency, mechanical load amplitude, and poling electric field strength were also studied to further characterize the composite material.

As the number of layers was varied from 1 to 9 with mechanical load amplitude of 1000 N and mechanical load frequency of 2 Hz, average maximum power was not significantly changed ($p<0.05$) and the optimal load resistance was lowered from 1 GΩ to 17 MΩ. When mechanical load frequency was increased from 1 to 5 Hz, the average maximum power for 9

layer implants with mechanical load amplitude of 1000 N increased from 551 μW to 2848 μW while shifting the optimal load resistance from 30 MΩ to 6 MΩ. Mechanical load amplitude was varied from 100 to 1000 N for 9 layer implants with mechanical load frequency of 2 Hz and resulted in average maximum power increasing from 8 μW to 1190 μW, with no significant effect on the optimal load resistance. Mechanical preload and poling electric field strength did not have a significant effect on either average maximum power or optimal load resistance.

The optimal load resistance was successfully lowered by approximately 3 orders of magnitude without significantly affecting the average maximum power generated by the specimen. Future work will develop circuitry needed for rectification and conditioning of the signal to deliver current densities which are delivered by devices currently in clinical use. Work will also continue to attempt to lower the optimal load resistance of the piezoelectric spinal fusion implants to improve performance with the developed circuitry.

Acknowledgements

I would like to thank the following people for their assistance, support, and time:

- Dr. Elizabeth Friis for her support and guidance throughout my time at KU. She has an infectious enthusiasm for developing and translating technologies to help others and without her hard work, this project would never have gotten to where it is.
- Dr. Lorin Maletsky and Dr. Kenneth Fischer for agreeing to be members of my thesis committee and for their assistance during my graduate career.
- John Domannm, Nick Tobaben, and Dr. Paul Arnold for their contributions to the piezoelectric spinal fusion project. Without their hard work, I would not have been able to contribute to this ongoing project.
- The Bioengineering Graduate Program and the Department of Mechanical Engineering have both given me the opportunity to further my education while working with great people.
- My lab-mates and friends Eric Tobaben, Erin Mannen, Kolton Stimpert, and Nikki Galvis for keeping me company, giving me advice, and always letting use them as a sounding board. You made my days in the lab enjoyable and kept me from losing my sanity during some of the longer days.
- My family for providing support and motivation that got me to where I am now.
- Krysta Gaiser for all of the support, sacrifice, and love that helped me get through graduate school. You are always there for me and I could not ask for anyone better by my side. You make my life truly special and I am blessed to have you.

This work was supported in part by the Institute for Advancing Medical Innovation

Table of Contents

List of Figures

List of Tables

Chapter 1. Background

The following chapter discusses the need for this work followed by the background knowledge which was needed for this work. First the relevant human anatomy will be discussed, followed by a discussion of existing spinal fusion techniques (including electrical stimulation of spinal fusion). Then the electromechanical properties of bone will be discussed and lastly the properties and theory of piezoelectric materials will be covered.

1.1. Problem Statement

Back pain is one of the most common causes for visits to the doctor in the US, with 70-85% of all people experiencing back pain at some point in their life. Back pain is also the most common cause of activity limitation in people younger than 45 years.[1] When back pain is caused by severe degeneration of the intervertebral disc, spinal fusion surgery is often used to alleviate pain and suffering due to collapsing discs, with over 600,000 fusion surgeries performed each year in the US. For patients who are classified as difficult-to-fuse (such as smokers and diabetics) failure rates for spinal fusion procedures without adjunct therapies have been reported as high as 29-46%.[2-6]

The most common adjunct therapies include bone morphogenetic proteins (BMPs) and DC electrical stimulation. BMPs have seen clinical success; however there have also been clinical issues with radiculitis, osteolysis, ectopic bone growth, and off-label treatments.[7-9] DC electrical stimulation has also seen clinical success, but has limitations. Longer surgeries are required because of the use of implantable battery packs, revision surgeries are sometimes necessary to remove the battery pack, and fusion does not occur in the interbody site.[10,11]

To address these issues a piezoelectric spinal fusion implant was developed which can produce electrical stimulation without the need for a battery pack. When attempting to improve power output from a piezoelectric material, the most power will be seen when the electrical load impedance is matched to the source impedance of the piezoelectric material. Piezoelectric materials are highly capacitive and thus during low frequency actuation (such as frequencies of 1-2 Hz in the human spine during walking) they have very high source impedances. To reduce this source impedance and thus make it easier to improve power output from piezoelectric materials, stacked actuators can be used.[12,13]

This work investigates the use of stacked actuators in a piezoelectric spinal fusion implant to improve the source characteristics of the implant. First, the effects of the number of layers on average maximum power output and the load resistance at which it occurred were investigated. The effects of mechanical preload, frequency and load amplitude on average maximum power and the load resistance at which it occurred were also investigated. Lastly, the effects of poling procedure on average maximum power and the load resistance at which it occurred were investigated.

1.1. Spine Anatomy

1.1.1. The Spine

The spine is composed of five main segments of vertebrae: coccyx, sacrum, lumbar, thoracic, and cervical, the last three of which contain 24 vertebrae. The seven most superior vertebrae are the cervical vertebrae, the next 12 most superior vertebrae are the thoracic vertebrae, and lastly the five most inferior (excluding the sacrum and coccyx) vertebrae are the lumbar vertebrae.[14]

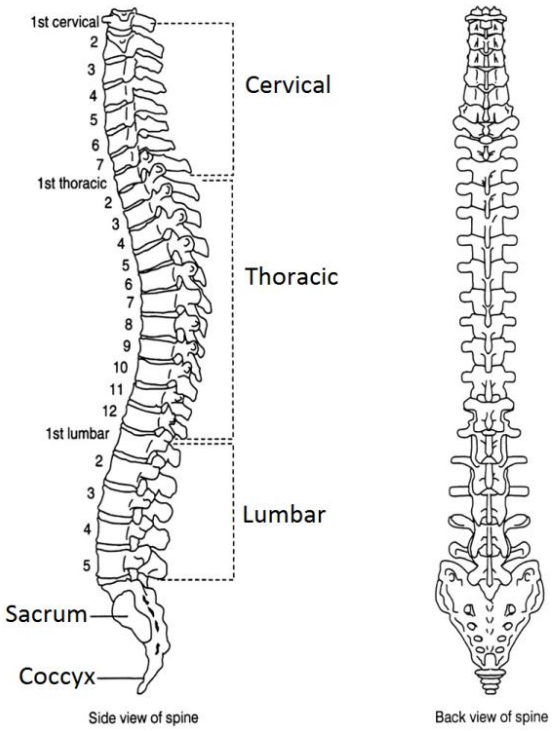

Figure 1. Anatomy of the Spine (Public Domain)

1.1.2. The Vertebrae

Each individual vertebrae consists of two main sections: the body and the processes. The body consists of the dense cortical rim and the less dense cancellous bone which it encases and is the primary load bearing portion of the vertebrae. The bone on the superior and inferior portions of the vertebral body, where the intervertebral disc rests, is called the end plate. The processes are the transverse process, the superior articular process, and the spinous process; these processes provide sites for attachment for the soft tissue and muscle to the spine. This section of the vertebrae also contains the pedicle and the lamina (a bony layer which protects the spinal cord).[14]

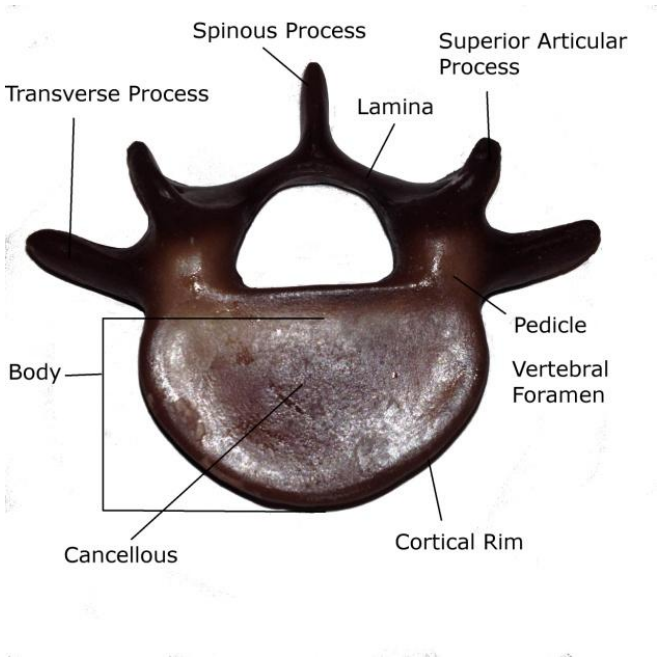

Figure 2. Anatomy of Vertebrae

1.1.3. The Intervertebral Disc

The intervertebral disc consists of the annulus fibrosus (the tough fibrous outer layer), the nucleus pulposa (the gel-like inner portion), and the lamellae (the outer collagenous layer). The nucleus pulposa bears most of the axial loads in the spine and also acts as a pivot point to allow the spine to pivot and flex. The annulus fibrosus and lamellae act together as a tough outer layer which forms a pressure vessel for the nucleus pulposus, containing it and providing structure. [14]

1.2. Spinal Fusion

1.2.1. Interbody Spinal Fusion

Initially, spinal fusion was done largely in the posterolateral space, first without, then with instrumentation.[15] Interbody lumbar fusion is based on the experiments by Bagby using a stainless steel basket in an equine model to hold autograph during fusion.[16-18] This experiment was a vast improvement on current techniques as it not only improved the survival rate of the

horses, but even allowed some of the horses to restore normal function.[18] Cloward first introduced posterior interbody lumbar fusion as a human treatment in 1953 and since the treatment (along with anterior interbody lumbar fusion) has been successfully used to fuse spinal segments.[15] Interbody fusion has the advantage of immediately stabilizing the segment initially with the cage and has shown potential to improve success rates of spinal fusions when compared to the posterolateral approach.[15,17]

1.2.2. Posterolateral Electrical Stimulation

While lumbar spinal fusion is clinically successful with reported rates of 90% or more for the healthy population, failure rates for those with multi-level fusions or high risk factors such as diabetes, obesity, or smoking, can be as high as 40%.[2,3,19] Electrical stimulation of spinal fusion has been used since 1974 to improve these rates.[19] Three main types of electrical stimulation are in use: direct current, capacitive coupling, and inductive coupling, the most widely used of which is direct current electrical stimulation.[19,20] Direct current electrical stimulation devices consist of a generator (a DC battery and circuitry hermetically sealed in a casing) and electrodes (typically made of titanium) which are placed along the transverse processes in contact with as much viable bone as possible. The generator is placed 5 to 8 cm away from the electrodes and acts as the anode. The electrodes (acting as the cathode) have an effective area of bone growth stimulation of 5 to 8 mm.[21] The stimulation provided by direct current electrical stimulation devices has been shown to increase fusion rates from 54%-80% in non-stimulated groups to 80-90% in stimulated groups.[2,19,21] Large scale analysis performed by Tian et al of 14 clinical studies of direct current electrical stimulation has shown that the overall success rate is 85% (95% CI, 76-91%).[20]

1.2.3. Interbody Electrical Stimulation

More recently electrical stimulation has been utilized in interbody fusion.[2,3] Electrical stimulation has been performed by using DC electrical stimulation through a titanium interbody cage using an ovine model with the goal of increasing the rate of fusion for these titanium interbody cages by Toth et al. Seven sheep were given BAK cages with no current applied, seven sheep were given BAK cages with 1.9 $\mu A/cm^2$, and eight sheep were given BAK cages with 4.7 $\mu A/cm^2$ (current densities that were less than and similar to, respectively, the current densities produced by DC stimulators in use at the time). Fusion was found to increase with increasing current density (using histologic assessment at 4 months); the non-stimulated group had a fusion rate of 29%, the group stimulated with 1.9 $\mu A/cm^2$ had a fusion rate of 71%, and the group stimulated with 4.7 $\mu A/cm^2$ had a fusion rate of 100%.[2]

Cook et al. performed similar experiments on primates with the primary goal of studying whether DC electrical stimulation of a titanium interbody fusion device with bone graft was more effective than titanium interbody fusion device with bone graft and without electrical stimulation. Cook et al. used 35 macaques, 10 with titanium interbody cages without electrical stimulation, 17 with titanium interbody cages with electrical stimulation, and 8 with femoral ring allograft. Significant improvement in the fusion rate was shown with electrical stimulation on radiographic assessment at 12 and 20 weeks. Fusion was achieved for 74% of the macaques at 12 weeks and 82% of the macaques at 20 weeks which received DC electrical stimulation achieved fusion, while only 40% of the macaques at 12 weeks and 43% of the macaques at 20 weeks which had not received DC electrical stimulation achieved fusion. The stimulated group was split into low current density stimulation (5.4 $\mu A/cm^2$) and high current density ($\mu A/cm^2$) with the high current density showing a higher fusion rate (80%) at 12 weeks than the lower current

density (33%). Samples sizes were only 5 high current density subjects and 3 current density subjects for 12 weeks however.[3]

Using electrical stimulation in the interbody space allows for targeted stimulation of bone growth, leading to improved efficacy of electrical stimulation procedures.

1.3. Electromechanical Properties of Bone

The direct and indirect piezoelectric effect in bone was measured by Fukada and Yasuda in 1957 using both human and ox femurs. They measured the piezoelectric constant of small square plates of bone which were boiled in hot water and then air dried. Their measurements showed that the piezoelectric constant was approximately 1/10th of that of quartz (a widely used, naturally occurring piezoelectric material).[22] Bassett and Becker published the results of a similar experiment in 1962; in this experiment they noted that when a bone was bent, areas under compression showed a negative potential when compared with those areas that were under tension (see Figure 3).[23] Wolff's Law had already established that bone adapts to the loads placed on it, but these experiments helped to explain how that adaptation can be controlled and directly lead to the first experiments using direct current electrical stimulation to induce bone growth.[23,24] It has also been found that there are larger field gradients in the vicinity of haversion canals than across a bulk sample, the magnitude of which are similar to those used in early electrical stimulation of bone growth. This field direction is directed to the haversion canals in areas under compression and away from the haversion canals in areas under tension, a small scale manifestation of the larger scale electrical gradient present during loading of bone.[25]

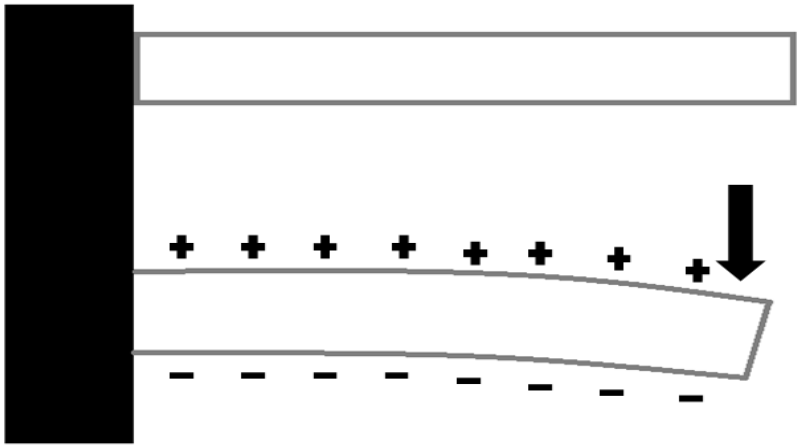

Figure 3. Relative charge of bone surfaces when a bending force is applied. (Adapted from Bassett et al.)[24]

1.4. Piezoelectric Materials

1.4.1. Basic Piezoelectric Theory

Piezoelectric materials are crystalline materials that exhibit both the direct and indirect piezoelectric effect. The direct piezoelectric effect is caused when a piezoelectric materials is put under an external pressure or stress which causes the electric dipoles within the material to align in such a way that the opposing faces of the material have opposite charges which in turn induces an electric field across the material. The indirect piezoelectric effect is the converse of the direct piezoelectric effect, that is, the material will deform when subjected to an electric field due to a displacement of electric dipoles within the material which in turn causes a strain proportional to the electric field.[26] For the piezoelectric or indirect piezoelectric effects to occur, piezoelectric materials must first be poled, a process which typically involves heating the material to a temperature near the curie temperature of the material and applying a strong electric field across the material, which causes the electric dipoles to reorient themselves in the direction of the electric field.[27]

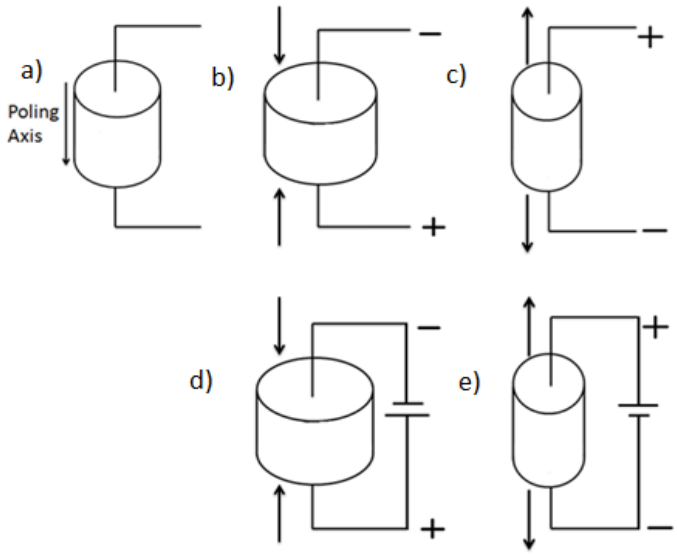

Figure 4. Piezoelectric effect for (a) Material at rest (b) Direct piezoelectric effect induced by compression and (c) tension (d) & (e) Indirect piezoelectric effect induced by opposite polarities. (Adapted from Mullinax et al.)[28]

1.4.2. Effect of Preload on Piezoelectric Actuators

Eichhorn et al. and Hu et al. looked at the effect of axial preload on piezoelectric actuators. Both groups showed that when a monolithic piezoelectric actuator is preloaded, it will change the resonant frequency and maximum power output of the actuator. As compressive axial preload increases, the resonant frequency decreases and the maximum power output increases. As tensile axial preload increases, the resonant frequency increases and the maximum power output increases. Table 1 shows the effects of preload on resonant frequency and maximum power output of monolithic piezoelectric elements (positive preload is compressive and negative preload is tensile).[29,30]

Table 1. Effects of preload on resonant frequency and maximum power output[30]

Preload (N)	Resonant Frequency (Hz)	Power Density (μW/cm^3)
-50	169.4	62
0	129.3	41
50	58.1	15

1.4.3. Poling Electric Field Strength

Law et al. studied the effects of electric field strength during the poling process on the d_{33} constant of PZT. All PZT ceramics were poled for 15 minutes at 125° C in an oil bath. The results in Figure 5 show that there is a steep increase in the value of the d_{33} piezoelectric coupling constant from 0-0.76 kV/mm and a weaker influence of electric field strength from 0.76-2 kV/mm.[31] The increase seen in the d_{33} constant indicates that the power output of these PZT ceramics also increased as the d_{33} constant is the primary determinant of changes in power output in through thickness actuation (with loading parameters held constant). Therefore it is important to ensure that the proper poling voltage is used to improve the power output of piezoelectric actuators.

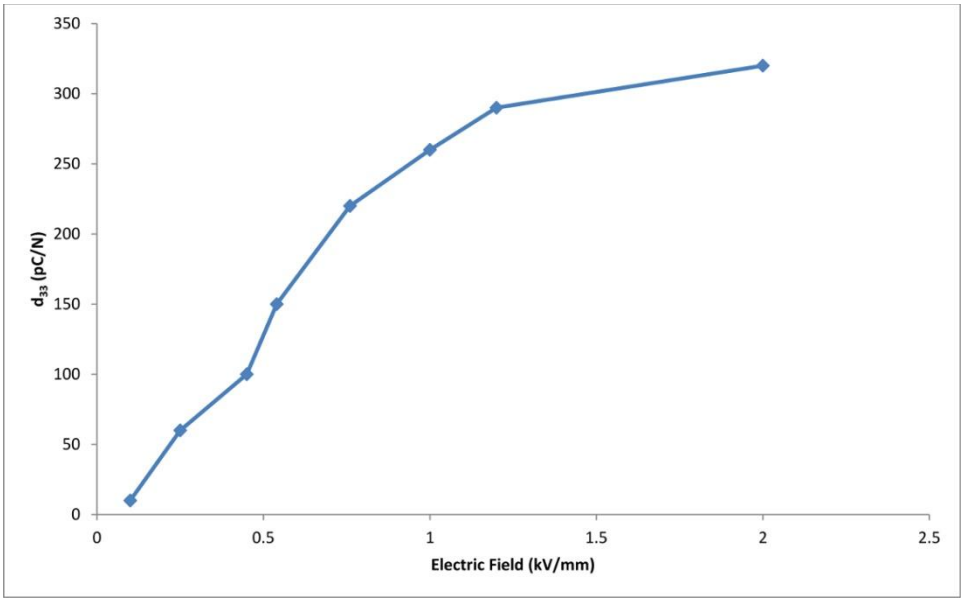

Figure 5. Effect of electric field strength on d_{33} constant. (Created using data from Law et al.)[31]

1.4.4. Stacked Piezoelectric Actuators

Piezoelectric elements are traditionally used as a single homogeneous material; however problems can arise with this when attempting to use them in power applications. The most prominent issue with using a single homogeneous element arises because it is important to match

impedance to get optimal power from piezoelectric materials, but these elements produce peak power outputs at resistive loads in the GΩ range. The resultant high peak voltages and low peak currents combined with the high impedance loads at which peak power occurs make these elements difficult to use to power circuits. One way to solve this problem is to use thin stacks of piezoelectric elements connected mechanically in series, but electrically in parallel (Figure 6). If the stacked elements and the single elements have the same geometry, they will produce the same power; however the stacked elements will produce that peak power at a much lower load resistance (optimal load resistance). Platt et al. were able to shift the optimal load resistance of a 10 mm x 10 mm x 18 mm stacked actuator composed of 145 layers of PZT ceramic from the GΩ range to the kΩ range.[12] Shenck et al. were able to produce a stacked actuator using 16 layers of PVDF which produced average raw power of 1.3 mW at a load resistance of 250 kΩ. The stacked actuator was placed in the insole of a shoe and loaded at 0.9 Hz walking pace. [13] [13] [13] [31] [31] [30] [29] [28] [27] [26] [25] [24] [23] [23] [23] [22] The successful implementation of stacked actuators will allow power to be generated at lower load resistance, simplifying the use of rectifying and conditioning circuitry.

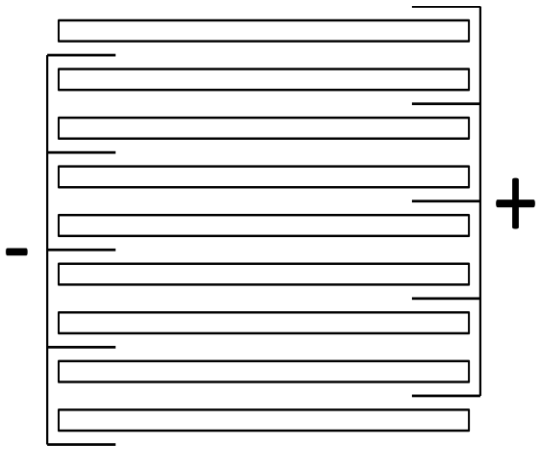

Figure 6. Diagram demonstrating how a stacked actuator is electrically connected. The top of each actuator is electrically connected to the bottom of the actuator below and the bottom of each actuator is connected to the top of the actuator below.

Chapter 2. Manuscript for Submission to JBMR Part A

The following is a manuscript formatted for submission to the Journal for Biomaterials Research Part A.

Composite piezoelectric spinal fusion implant: effects of stacked actuators

ABSTRACT

Spinal fusion surgeries have a high failure rate for difficult-to-fuse patients. A piezoelectric spinal fusion implant was developed to overcome the issues with other adjunct therapies. Stacked actuators were used to improve power generation at low electrical load resistances. The effects of the number of layers on average maximum power and the load resistance at which that average maximum power occurred (optimal load resistance) were studied. The effects of mechanical preload, mechanical loading frequency, mechanical loading amplitude, and poling procedure were also studied. Increasing the number of layers from one to nine was found to lower the optimal load resistance from 1.00 GΩ to 16.78 MΩ while not significantly affecting average maximum power. Mechanical preload and poling procedure did not have a significant effect on power output or optimal load resistance. Increases in mechanical loading frequency increased average maximum power, while lowering the optimal load resistance. Increases in mechanical loading amplitude increased average maximum power output without affecting the optimal load resistance.

KEYWORDS

spine, fusion, interbody, electrical stimulation

INTRODUCTION

In the United States, back pain is one of the most common reasons for physician appointments and was the third most prevalent cause of surgeries in 1990[1] In those cases which result in surgery to alleviate lower back pain, lumbar spinal interbody fusion is a commonly performed procedure with over 600,000 fusion operations done in the USA each year. However, in instances where the patient is classified as difficult-to-fuse (for example, diabetics and smokers) failure rates for this procedure without the use of adjunct therapies have been reported as high as 29-46%.[2-6]

The most widely used adjunct therapies that help stimulate bone healing to address this high failure rate are bone morphogenetic proteins and electrical stimulation. Bone morphogenetic proteins have shown good results in stimulating bone growth, but there have been clinical issues with ectopic bone growth, osteolysis, radiculitis, and off-label treatments.[7-9] Electrical stimulation for bone healing is accomplished internally or externally. External electrical stimulators are noninvasive and function by generating electromagnetic fields to promote bone healing. These devices have issues with user compliance because they are dependent on users wearing them for a given number of hours. Internal electrical stimulation operates using direct current (DC) stimulation applied to an electrode implanted at the site of desired fusion. Currently available DC internal stimulation devices utilize titanium electrodes which are placed along the transverse processes and have an implantable battery pack placed in the soft tissue 5-8 cm away from the site of stimulation.[21] These implantable DC internal stimulation devices have shown clinical success in promoting fusion, but it has drawbacks in that the fusion is not at the interbody site, it must be used at the time of initial surgery, use of the implantable battery pack leads to longer surgery times (compared to the same spinal fusion procedures without the battery

pack), and a second surgery may be required to remove the battery pack.[10,11] Current adjunct therapies all require substantial additional cost beyond the baseline fusion device and surgical procedure that may or may not be covered by healthcare insurance.

The problems with current techniques was a motivation for the development of a piezoelectric interbody spinal fusion implant in which DC electrical stimulation for bone healing in the interbody space is achieved by loading of the implant between two vertebrae through the natural motion of the human body. Piezoelectric materials produce electric charge in response to mechanical stress; most piezoelectric materials are brittle and stiff ceramics. Piezoelectric composite materials allow for a tough material to serve as a load-bearing structure. Use of a piezoelectric composite material in a spinal fusion interbody implant allows for delivery of current to an attached electrode on the device surface generation of a current when the implant is being compressed during normal body functions.

Theoretical electromechanical computational models have shown that it would be possible to generate current densities in the range of those currently used in implantable DC electrical stimulation devices with a 9 mm thick implant made with a 1-3 piezoelectric composite material. However, at the relatively low frequency ranges seen in the human body, this implant design was shown to deliver this peak current density at a load impedance in the GΩ range, far above the load impedances present in the body that are typically in the kΩ range.[32,33] Piezoelectric materials are high-voltage, low-current sources at low frequencies with high source impedances which are almost purely capacitive.[12,13]

A technique that is used in piezoelectric technologies is to stack thin layers of piezoceramic materials alternated with electrodes. The electrical energy produced by a multiple layer piezoceramic has a much lower associated voltage and significantly higher current than that

of a single-layer piezoceramic structure. Shenck et al. were able to produce 1300 μW of RMS average, raw power using 3-1 mode actuation of a 16 layer PVDF stave placed under the insole of a standard Nike sneaker at a 250 kΩ load resistance with a mechanical loading frequency of 0.9 Hz. The voltage output was measured across matched resistive loads at a brisk walk.[13] Platt et al. were also successful in generating 1080 μW of average, raw power with a 145 layer PZT stack with a 14.8 kΩ load resistance, a mechanical loading frequency of 1 Hz , and a mechanical load amplitude of 800 N.[12] The power produced in both of these experiments are an order of magnitude higher than the power needed to produce the current densities seen in implantable DC electrical stimulation devices which are currently in use (4-5 $\mu A/cm^2$), assuming electrode surface area is held constant.[32]

In the present study, the ability to generate power with 1-3 piezoelectric stacked layer composite was investigated. The influence of the number of layers, preload, and load frequencies normally experienced in the body across a range of impedances was measured.

MATERIALS AND METHODS

Implant Design

The first design of the composite implants was in preparation for preliminary animal trials, so the initial design of the implant was based on the overall geometry of 18x10x10 mm used by Krijnen et al. for goat studies of a spinal fusion implant.[34,35] The theoretical model developed by Tobaben et al., which used a lumped parameter model of the mechanical system in developing a circuit model (Figure 7) of piezoelectric composites, was adapted to predict how the change in the number of layers would affect the peak power produced by the implant and the load resistance at which that peak power would occur (herein referred to as optimal load

resistance).[32] This model predicted that the peak power would remain constant and that the optimal load resistance could be shifted from approximately 2 GΩ to approximately 9 MΩ (Figure 8). Numbers of layers of 1, 3, 6, and 9 were chosen to be manufactured because of the practical limitations of cutting slices less than 1 mm thick and diminishing returns seen as the number of layers per implant was increased.

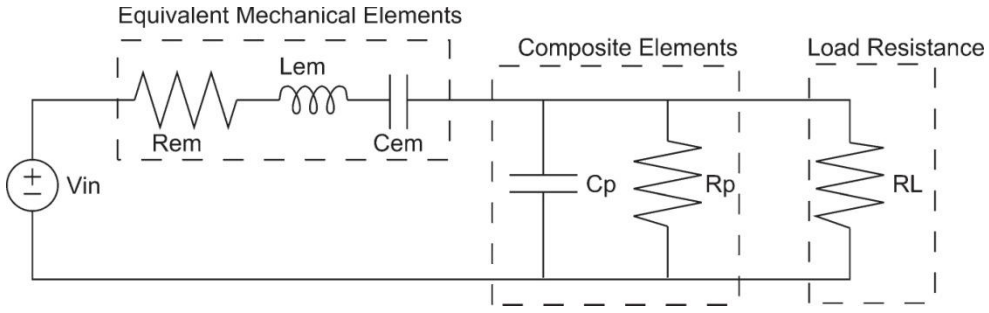

Figure 7. Piezoelectric Composite Circuit Model

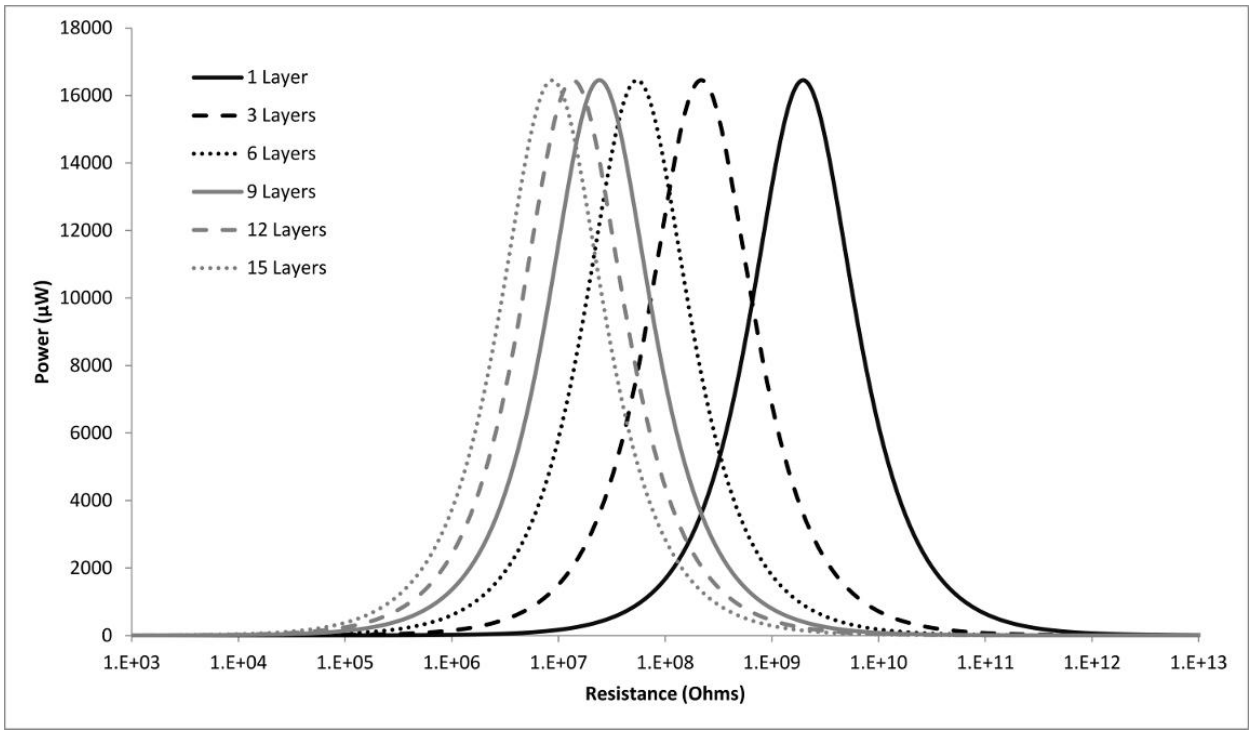

Figure 8. Results of theoretical analysis of predicted change in power with variations in number of layers

Specimen Fabrication

Piezoelectric 1-3 composite columns were constructed using 800 μm diameter PZT 5A fibers (Smart Materials Corp., Sarasota, FL) in a medical grade epoxy (EPO-TEK 301, Epoxy Technology Inc., Billerica, MA) matrix. EPO-TEK 301 was chosen as the matrix material for both its handling characteristics and material properties. It is a room temperature cure two part thermoset epoxy, which makes it easy to work with in a laboratory setting. EPO-TEK 301 also has compressive modulus and strength comparable to PEEK and reasonable electrical properties. It has been used previously in load-bearing medical applications and is compliant with USP Class VI Biocompatibility standards.[36-38] The piezoelectric fiber material, PZT 5A1, was chosen because of the favorable piezoelectric charge coefficient (440 C/N).[39] The composite columns were constructed with a surface area of 75 mm^2, a height of 100 mm, and a PZT fiber volume fraction of 23.2%. The overall geometry of the specimens was based on the implant shape used by Krijnen et al. in goat lumbar fusion studies. The cross-section shape (Figure 9) used was modified slightly to be similar to "bullet" implants used in current posterior lumbar interbody spinal fusion procedures.[34,35]

The composite columns were then cut using a diamond blade saw into 1 mm, 1.5 mm, 3 mm, and 9 mm slices to assemble stacked specimens with 9 layers (n=5), 6 layers (n=3), 3 layers (n=5), and 1 layer (n=6), respectively. Individual layers were sputter coated with a 100 nm thick layer of gold on top and bottom to ensure electrical connectivity between all fibers in each layer. Individual layers were then stacked and wired as shown in Figure 10 such that they were connected electrically in parallel but mechanically in series. Electrical connections were made using conductive adhesive back copper tape and EPO-TEK 301 was used to mechanically bond layers together. All epoxy was allowed to cure at room temperature for at least 24 hours prior to poling.

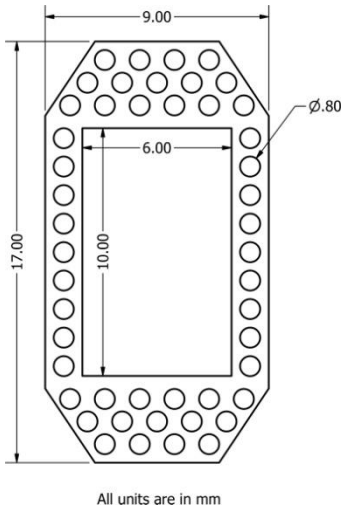

Figure 9. Cross section and fiber layout of specimens

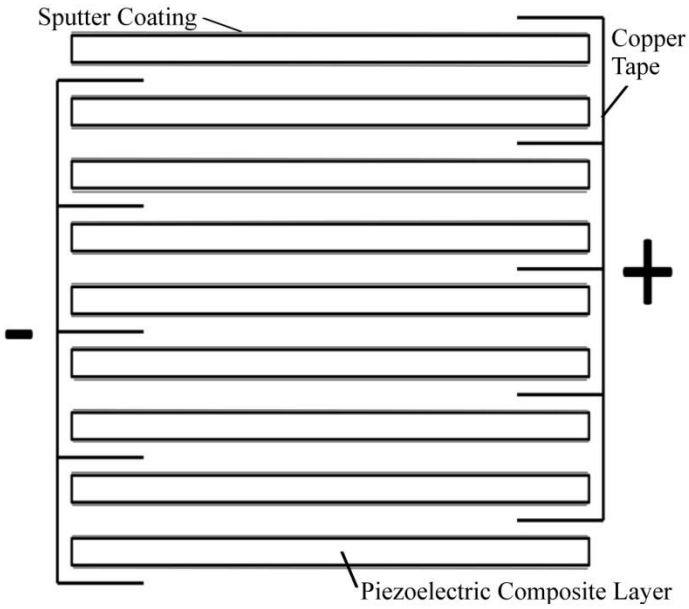

Figure 10. Exploded view of electrical connection between a 9 layer specimen. Note that copper tape is adhered to sputter coating on the surface of the composite layers

Electromechanical Testing

Each specimen was tested using two different procedures. Before testing, each specimen was poled at 1 kV/mm for 30 minutes per lab protocol, with the exception of the 9 layer specimen during the testing of the effects of preload, which were poled at 2 kV/mm for 15 minutes. The poling procedure was changed to compare the effects of poling at 2 kV/mm to

poling at 1 kV/mm after the instructions for poling at 2 kV/mm were added to the manufacturer's website.[40] The first test procedure measured the voltage output of each specimen at 38 load resistances ranging from 420 kΩ to 5 GΩ under a compressive 1200 N preload to peak-to-peak load amplitudes of 100, 500, and 1000 N and at loading frequencies of 1, 2, 3, and 5 Hz. The load amplitudes were chosen to be representative of loads expected in the intervertebral space after a spinal fusion surgery with instrumentation.[32] Loading frequencies were representative of the range of normal human motion.[41] The second testing procedure measured the voltage output of each sample at 5.11 kΩ, 9.94 kΩ, 94.06 kΩ, and 16.76 MΩ with compressive preloads of 200, 400, 600, 800, 1000, and 1200 N (with a load amplitude of 100 N) and a constant loading frequency of 2 Hz. Saha et al. found the average resistivity of cortical bone to be 1.55 kΩ-cm and the average specific capacitance to be 33.81 pF/cm when measured at 100 kHz. The load resistances of 5.11 kΩ, 9.94 kΩ, and 94.06 kΩ were chosen to be similar to tissue resistances found by Saha et al. The circuit was set up as seen in Figure 1, with voltage measurements taken across the resistive load. Preloads were varied from 200 N to 1200 N. The loading frequency of 2 Hz was chosen as a normal gait frequency.[41] Fifteen force loading cycles were collected at 512 Hz for all force amplitudes, frequencies, and load resistances using an MTS MiniBionix 858 (MTS Corp., Eden Prairie, MN) using a 2.5 kN load cell. All 20 specimens were tested using both protocols, with the exception of one of the three layer specimens, as it was accidentally damaged after the first testing procedure was completed.

Raw voltage measurements were collected and then that data was analyzed using MATLAB. Voltage data was rectified after shifting the DC voltage offset to 0 V. The first 2.5 and last 2.5 cycles were then dropped from the data set to avoid spikes in the data due to initial loading and unloading. Average maximum voltage was then calculated by taking the average of

the maximum voltage during each loading cycle to which the specimen was subjected. The average maximum voltages were used to determine the average maximum power seen by the load resistors using the known load resistance values and Joule's Law ($P=V^2/R$). The statistical evaluation of all results was performed in MATLAB. Evaluation of the statistical significance of comparisons of the effects of preload, frequency, load amplitude, and poling procedure were done using matched pair t-tests. Evaluation of the statistical significance of comparisons of the effects of the number of layers in the specimen was done using unequal variance, two sample t-tests. Power analysis of data was performed post hoc using the sampsizepwr function in MATLAB. The sample mean was used for the mean under the alternative hypothesis.

RESULTS

The effects of preload, load amplitude, frequency, poling procedure used, and number of layers on power over a range of load resistances was measured. The majority of comparisons had a power of 0.9 or greater; 83.5% of the comparisons had a power of 0.9 or greater and 90.6% of the comparisons had a power of 0.8 or greater.

As expected, varying preload did not significantly change the average maximum power produced by the specimens ($p<0.05$). Table 2 shows the effects of load amplitude on average maximum power output of 9 layer specimen at 1200 N preload and 2 Hz. Increasing load amplitude with a given preload resulted in significant increases in average maximum power generation($p<0.05$). Figure 11 shows the relationship of power across load resistances for the 9 layer specimens tested at 1000 N load amplitude at 1, 2, 3 and 5 Hz. Increases in frequency increased the peak power produced while significantly lowering the optimal load resistance of

the generator ($p<0.05$). The change in voltage due to different poling electric field strengths was not significant ($p=0.10$).

Figure 12 shows average data from testing the 1, 3, 6 and 9 layer specimens with the same overall volume fraction of piezoelectric fibers at 2 Hz, 1000 N load amplitude, and 1200 N preload. Average maximum power obtained and optimal load resistance with respect to the number of layers in the specimen can be seen in Table 3. The optimal load resistance was significantly decreased with an increase in the number of layers ($p<0.05$), however, as predicted by the computational model, maximum power was not significantly influenced by the number of layers. Figure 13 shows a nonlinear relationship of voltage output over a lower range of load resistances. An increase in the number of layers of the specimen resulted in significantly higher voltage levels for a given load resistance ($p<0.05$).

Table 2. Comparison of the effects of load amplitude on power output of 9 layer specimens at 2 Hz

Load Amplitude (N)	Average Maximum Power (μW)
100	8.2
500	260.9
1000	1189.5

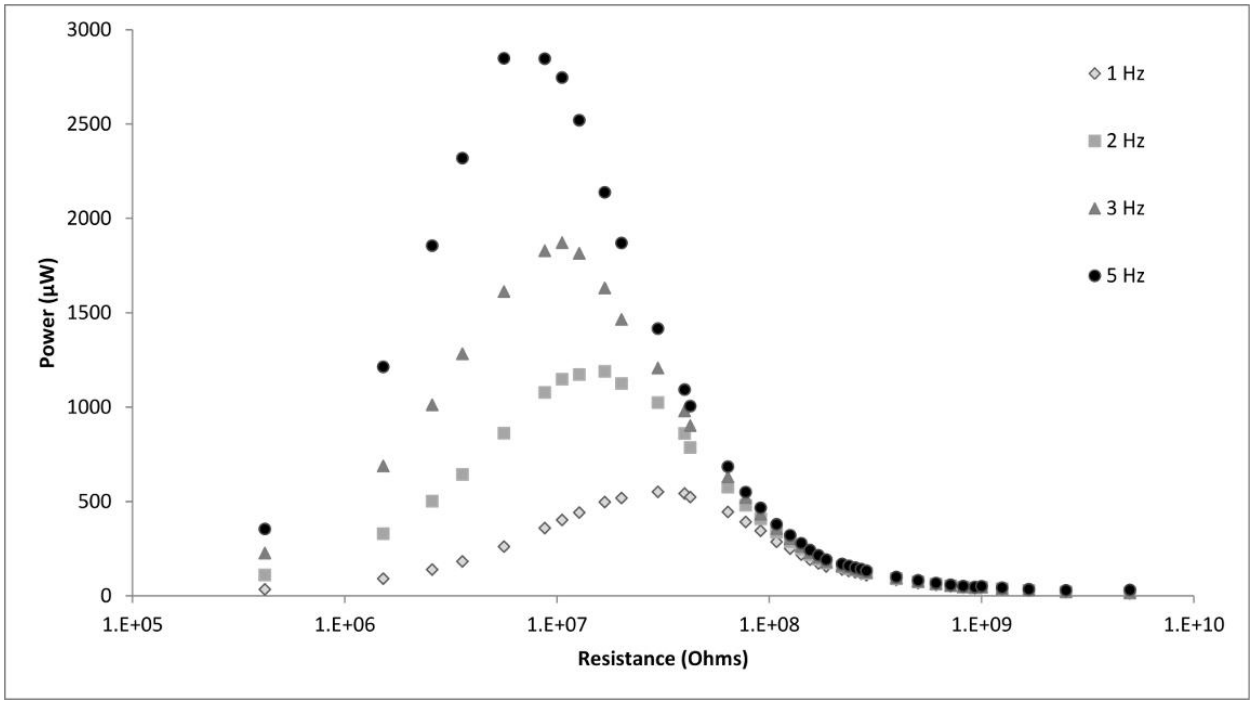

Figure 11. Comparison of the effects of frequency on power output of 9 layer specimen at 1000 N load amplitude

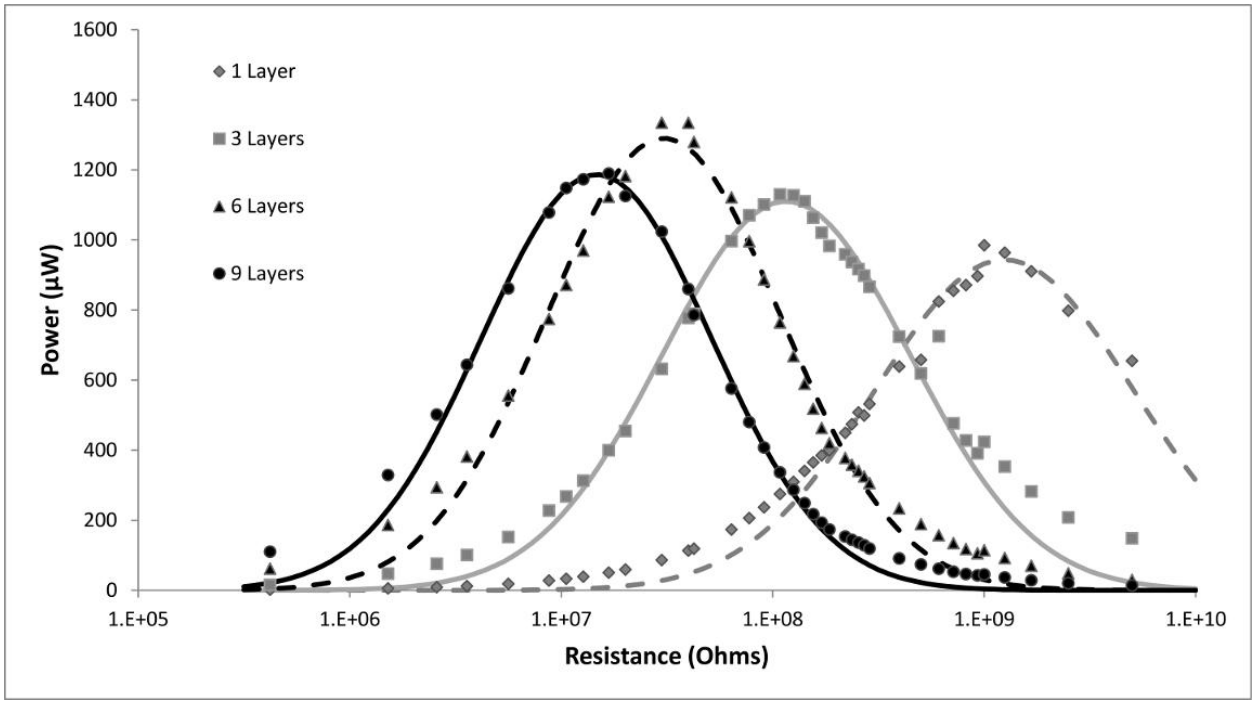

Figure 12. Comparison of the effects of varying number of layers on power output of layered specimen at 1000 N force amplitude and 2 Hz load frequency. Data is averaged across all specimen of a given thickness,

error bars excluded for visual clarity Lines representing a Gaussian fit of each data set predict the optimal load resistance for each specimen type.

Table 3. Average maximum power and optimal load resistance measured with respect to the number of layers.

Number of Layers	Average Maximum Power (μW)	Optimal Load Resistance (MΩ)
1	984±314	1000.42
3	1130±452	108.22
6	1135±475	29.87
9	1189±439	16.78

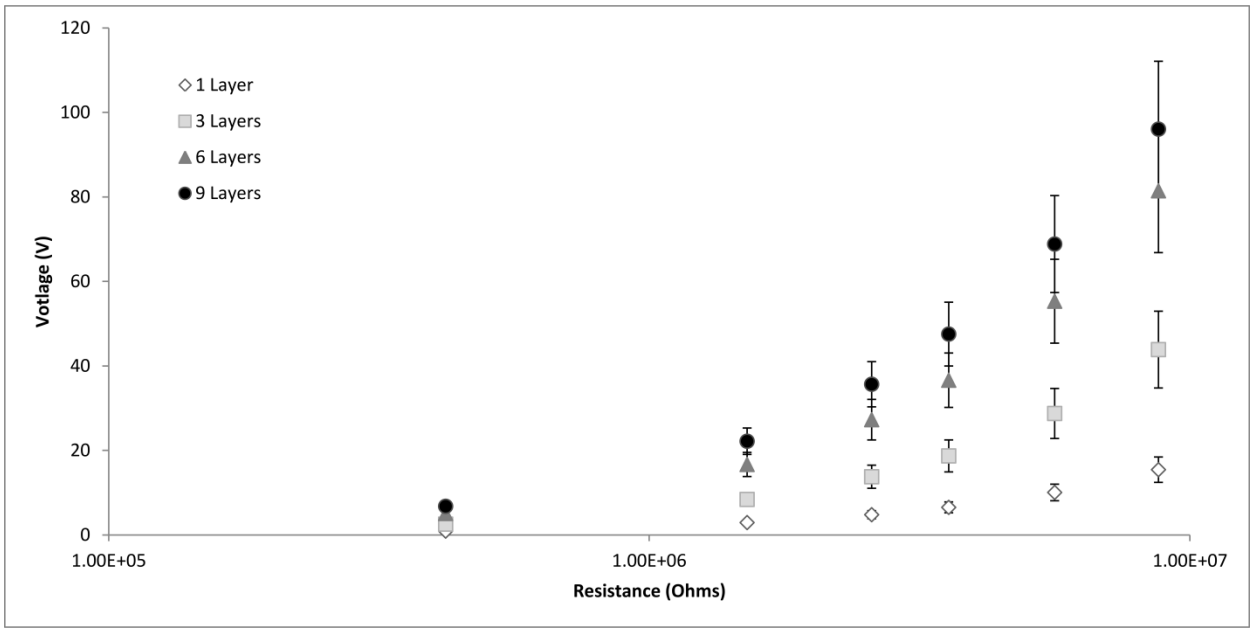

Figure 13. Voltages generated by 1, 3, 6, and 9 layer specimens at lower resistances

DISCUSSION

The purpose of this study was to determine the feasibility of using a layered design (that is, stacked actuator) to shift the optimal load resistance of a piezoelectric lumbar interbody spinal fusion implant made from a 1-3 PZT-epoxy composite. Shifting of the optimal load resistance has been successfully implemented by Shenck and Platt using stacks of monolithic actuators.[12,13]

A computational model predicted that this technique would lower the optimal load resistance of a 1-3 composite from approximately 2 GΩ to approximately 24 MΩ, as the number of layers was increased from one to nine. It was also hypothesized that as with monolithic piezoelectric materials, changing the preload applied to layered 1-3 composites would not significantly influence power generation at low frequencies and that the maximum power generated would increase with an increase in either load amplitude or load frequency.

The results of average peak power comparisons between specimens with different numbers of layers showed that the optimal load resistance was decreased from 1.00 GΩ to 16.78 MΩ as the number of layers was increased from one to nine, agreeing in general with theoretical predictions. The average peak power generated from all of the specimens at 1200 N preload, 1000 N load amplitude, and 2 Hz was approximately 1132 μW. The power generated is an order of magnitude lower than the predicted power output from the theoretical model using the same parameters, possibly due to several factors including fiber misalignment within layers, differences between material and electrical properties used in the theoretical model and actual material and electrical properties, and issues with the interface between the PZT fibers and the matrix epoxy. The power generated by the specimens is still in excess of the power needed to directly produce the current density seen in current electrical stimulation devices. However, not all power generated would be available to produce current densities seen in clinically-used electrical stimulation devices. Present day clinically used DC electrical stimulation and are therefore able to deliver a constant electronegative stimulation without rectification.[33] The piezoelectric implants generate an AC signal and thus must be rectified and conditioned using appropriate circuitry to ensure that proper electronegative stimulation with the appropriate current density levels is delivered. Depending on circuit design, these rectifying and regulating

circuits could use a substantial portion of the power generated. Future work must include this consideration in implant design.

Work done by Eichhorn and Hu has shown that varying preloads will affect the power output of piezoelectric elements at a constant frequency by changing both the resonant frequency and the maximum power produced by piezoelectric elements.[29,30] However, the resonant frequencies for most piezoelectric materials are well above 100 Hz, thus the effects of the change in preload are negligible during low frequency actuation. The effects of preload will continue to be negligible for this application as most loading of a spinal fusion cages at frequencies below 5 Hz.

Piezoelectric materials are essentially capacitive, and because of this increasing load frequency lowers the optimal load resistance and increase the peak power output of piezoelectric stack actuators.[12] The results seen in Figure 3 show that this held true for composite piezoelectric stack actuators. Future work will need to focus on even lower frequencies than 1 Hz, as the typical gait frequency range for walking and higher frequency loading of the spine will be inconsistent, especially with limitations placed on patient activity while recovering from spinal fusion surgeries.[42] The increases in load amplitude lead to increased power output, as demonstrated by the equations which govern piezoelectric material behavior, which show that electric field strength output by the piezoelectric material is proportional to the applied force.[12]

The load resistance of body tissue in the interbody space is not well defined. Measurements of bone resistivity and specific capacitance, such as those taken by Saha et al, give some indication of the body tissue load resistance.[43] Other measurements have been taken of load resistance in the spine, but not in the interbody space.[33] Future work will need to further investigate the load resistance in the interbody space while accounting for soft tissue and fluid.

The matrix material used to produce the implants can be changed for future work to other materials which are suitable for injection molding. A prime candidate for a new matrix material is PEEK as it is currently widely used in spinal fusion implants and it should provide mechanical and electrical performance similar to the current matrix material, EPO-TEK 301. This would not significantly change the overall production process, although it would require manufacturing expertise with high temperature injection molding.

Future work could also include increasing the number of layers in a given implant thickness. In the present study, attempts were made to manufacture a 15 layer specimen. Unfortunately, the mechanical attachment of the piezoelectric fibers to the epoxy matrix was not sufficient to retain the fiber in the matrix during cutting of the sections when thinner than one mm thick. To allow for thinner slices that retain mechanical attachment, future work should improve fiber-matrix interface strength.

CONCLUSIONS

The successful implementation of a piezoelectric spinal fusion implant can help difficult-to-fuse patients by improving success rates (compared to spinal fusion without adjunct therapies), removing financial cost and physical discomfort associated with removal of DC electrical stimulators, and by improving surgery time and ease compared with DC electrical stimulators. The use of a stacked actuator with the 1-3 PZT-epoxy composite designed to be similar in size and shape as piezoelectric lumbar interbody fusion implants successfully lowered the optimal load resistance from the GΩ range to the MΩ range. The power required to deliver necessary current density to the electrodes will be dictated by circuit design. Actual load resistances in the interbody space experienced by an interbody device should be measured. Future work will focus on further lowering the optimal load resistance of the piezoelectric

composite so that more power can be produced at load resistances which are feasible for use with rectifying and signal conditioning circuitry.

ACKNOWLEDGEMENTS

This research was supported by the Institute for Advancing Medical Innovation. The authors would also like to thank Michael Latham for his assistance in manufacturing the specimens.

Chapter 3. Conclusions and Future Work

The optimal load resistance of the piezoelectric spinal fusion implant was successfully lowered from 1.00 GΩ to 16.78 MΩ by changing the number of layers in the implant from 1 to 9 without significantly affecting average maximum power output. Mechanical load amplitude increased average maximum power as it increased without significantly affecting optimal load resistance. As frequency increased, optimal load resistance decreased and average maximum power increased. Preload and poling electric field strength did not significantly affect average maximum power output or optimal load resistance.

Future work will focus on increasing power output of the piezoelectric spinal fusion implant at lower load resistances by further lowering the optimal load resistance and improving material properties. The power needed from the piezoelectric spinal fusion implant will be dependent on the power needed to generate appropriate current densities for DC electrical stimulation and on the power needed to operate rectifying and conditioning circuitry to deliver regulated, electronegative stimulation to the fusion site. Work will also need to be done on using a matrix material (such as PEEK) which will be clinically accepted.

References

1. Andersson GB. Epidemiological features of chronic low-back pain. Lancet 1999;354(9178):581-5.
2. Toth JM, Seim HB, 3rd, Schwardt JD, Humphrey WB, Wallskog JA, Turner AS. Direct current electrical stimulation increases the fusion rate of spinal fusion cages. Spine (Phila Pa 1976) 2000;25(20):2580-7.
3. Cook SD, Patron LP, Christakis PM, Bailey KJ, Banta C, Glazer PA. Direct current stimulation of titanium interbody fusion devices in primates. Spine J 2004;4(3):300-11.
4. Kane WJ. Direct current electrical bone growth stimulation for spinal fusion. Spine (Phila Pa 1976) 1988;13(3):363-5.
5. Kucharzyk DW. A controlled prospective outcome study of implantable electrical stimulation with spinal instrumentation in a high-risk spinal fusion population. Spine (Phila Pa 1976) 1999;24(5):465-8; discussion 469.
6. Meril AJ. Direct current stimulation of allograft in anterior and posterior lumbar interbody fusions. Spine (Phila Pa 1976) 1994;19(21):2393-8.
7. Epstein NE. Pros, cons, and costs of INFUSE in spinal surgery. Surg Neurol Int 2011;2:10.
8. Epstein NE, Schwall GS. Costs and frequency of "off-label" use of INFUSE for spinal fusions at one institution in 2010. Surgical neurology international 2011;2.
9. Carragee EJ, Hurwitz EL, Weiner BK. A critical review of recombinant human bone morphogenetic protein-2 trials in spinal surgery: emerging safety concerns and lessons learned. Spine J 2011;11(6):471-91.
10. An HS, Lynch K, Toth J. Prospective comparison of autograft vs. allograft for adult posterolateral lumbar spine fusion: differences among freeze-dried, frozen, and mixed grafts. Journal of Spinal Disorders & Techniques 1995;8(2):131-135.
11. Glazer PA, Glazer LC. Electricity: the history and science of bone growth stimulation for spinal fusion. Orthop J Harvard Med School Online 2002;4:63-67.
12. Platt SR, Farritor S, Haider H. On low-frequency electric power generation with PZT ceramics. Mechatronics, IEEE/ASME Transactions on 2005;10(2):240-252.
13. Shenck NS, Paradiso JA. Energy scavenging with shoe-mounted piezoelectrics. IEEE Micro 2001;21:30-42.
14. Pruitt LA, Chakravartula AM. Mechanics of Biomaterials: Fundamental Principles for Implant Design: Cambridge University Press; 2011.
15. Tehranzadeh J, Ton JD, Rosen CD. Advances in spinal fusion. 2005. Elsevier. p 103-113.
16. Zdeblick TA, Phillips FM. Interbody cage devices. Spine (Phila Pa 1976) 2003;28(15 Suppl):S2-7.
17. Blumenthal SL, Ohnmeiss DD, Nass. Intervertebral cages for degenerative spinal diseases. Spine J 2003;3(4):301-9.
18. McAfee PC. Current Concepts Review-Interbody Fusion Cages in Reconstructive Operations on the Spine*. The Journal of Bone & Joint Surgery 1999;81(6):859-80.
19. Gan JC, Glazer PA. Electrical stimulation therapies for spinal fusions: current concepts. Eur Spine J 2006;15(9):1301-11.
20. Tian NF, Wu YS, Zhang XL, Mao FM, Xu HZ, Chi YL. Efficacy of electrical stimulation for spinal fusion: a meta-analysis of fusion rate. Spine J 2013;13(10):1238-43.

21. Kahanovitz N. Electrical stimulation of spinal fusion: a scientific and clinical update. Spine J 2002;2(2):145-50.
22. Fukada E, Yasuda I. On the piezoelectric effect of bone. Journal of the Physical Society of Japan 1957;12(10):1158-1162.
23. Bassett CA, Becker RO. Generation of electric potentials by bone in response to mechanical stress. Science 1962;137(3535):1063-4.
24. Bassett CA. Electrical effects in bone. Sci Am 1965;213(4):18-25.
25. Hastings GW, Mahmud FA. Electrical effects in bone. J Biomed Eng 1988;10(6):515-21.
26. Vijaya S. Piezoelectric Materials and Devices: Applications in Engineering and Medical Sciences: Taylor & Francis; 2012.
27. Sodano HA, Inman DJ, Park G. A review of power harvesting from vibration using piezoelectric materials. Shock and Vibration Digest 2004;36(3):197-206.
28. Mullinax D, Guy J, Koprowski R, Laczko M. Harvesting the energy from friction to create a safer bike. 2013.
29. Eichhorn C, Goldschmidtboeing F, Woias P. Bidirectional frequency tuning of a piezoelectric energy converter based on a cantilever beam. Journal of Micromechanics and Microengineering 2009;19(9):094006.
30. Hu Y, Xue H, Hu H. A piezoelectric power harvester with adjustable frequency through axial preloads. Smart materials and structures 2007;16(5):1961.
31. Law H, Rossiter P, Simon G, Unsworth J. A model for the structural hysteresis in poling and thermal depoling of PZT ceramics. Journal of materials science 1995;30(19):4901-4905.
32. Tobaben NE, Domann JP, Arnold PM, Friis EA. Theoretical model of a piezoelectric composite spinal fusion interbody implant. J Biomed Mater Res A 2014;102(4):975-81.
33. Biomet. Implantable spinal fusion simulators physician's manual & full prescribing information SpF PLUS-Mini, SpF-XL IIb. http:==www.biomet.com=spine=getFile.cfm?id52889&rt5inline.; 2009.
34. Krijnen MR, Mullender MG, Smit TH, Everts V, Wuisman PI. Radiographic, histologic, and chemical evaluation of bioresorbable 70/30 poly-L-lactide-CO-D, L-lactide interbody fusion cages in a goat model. Spine (Phila Pa 1976) 2006;31(14):1559-67.
35. Smit TH, Krijnen MR, van Dijk M, Wuisman PI. Application of polylactides in spinal cages: studies in a goat model. J Mater Sci Mater Med 2006;17(12):1237-44.
36. International A. Materials and Coatings for Medical Devices: Cardiovascular: ASM International; 2009.
37. Incorporated ET. EPO-TEK 301 Technical Data Sheet. 2012.
38. Products QEP. Quadrant EPP Ketron 1000 PEEK Polyetheretherketone, unfilled, extruded (ASTM Product Data Sheet)
39. 5A1, 5H2 Typical Material Properties. Smart Material Corporation; 2014.
40. Corporation SM. Typical PZT Fiber ordering and availability data. 2014.
41. Pachi A, Ji T. Frequency and velocity of people walking. Structural Engineer 2005;83(3).
42. Cromwell R, Schultz AB, Beck R, Warwick D. Loads on the lumbar trunk during level walking. J Orthop Res 1989;7(3):371-7.
43. Saha S, Williams PA. Electric and dielectric properties of wet human cortical bone as a function of frequency. Biomedical Engineering, IEEE Transactions on 1992;39(12):1298-1304.

Appendix A. Materials and Methods

The first design of the implants was in preparation for preliminary animal trials, so the initial design of the implant was based on the overall geometry used by Krijnen et al. for goat studies of a spinal fusion implant.[34,35] This design, shown in Figure 14, was then modified to resemble some bullet shaped spinal fusion implants currently used in posterior lumbar interbody fusion (PLIF). The implant was designed so that it had an internal insert containing the composite actuator that was incased in 0.5 mm of epoxy on all sides, due to concerns of PZT wear on the top and bottom surfaces. This experiment tested specimens which were 9 mm tall without the incasing epoxy.

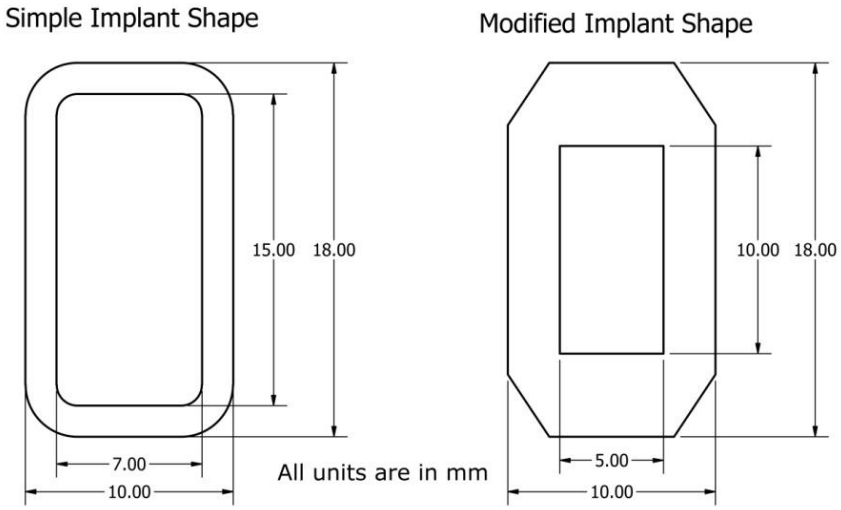

Figure 14. Comparison of implant shape used by Krijnen et al (left) and the modified implant shape used in the current work

The distribution of the specimens specimens created can be seen in Table 4. Columns were made using the implant insert cross-sectional geometry, but approximately 100 mm tall. Forty-eight PZT 5A (Table 4)rods of 800 μm diameter (Smart Materials Corp, Sarasota, FL) placed longitudinally throughout the column embedded in a matrix material of EPO-TEK 301 (Epoxy Technology Inc, Billerica, MA). Figure 15 shows a cross section view of these columns.

These columns were allowed to cure at room temperature for 24 hours and then sliced into the needed number of layers of appropriate thickness (Table 5) using a diamond blade saw. Both sides of each layer were coated with a 100 nm thick layer of gold. Layers were then assembled so that the specimens were stacked mechanically in series, but were connected electrically in parallel (Figure 16). These layers were connected electrically using copper tape, with EPO-TEK 301 used to mechanically bind the specimens together. These specimens were placed on an aluminum post to ensure proper alignment while they were allowed to cure at room temperature for 24 hours.

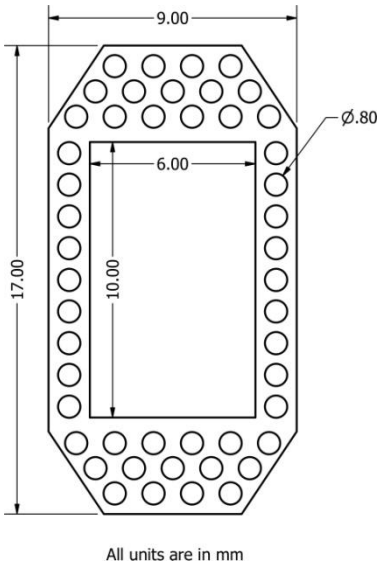

Figure 15. Cross section and fiber layout of specimens

Table 4. Properties of PZT 5A1

PZT Type	5A1
Fiber Diameter (μm)	800
d_{33} ($x10^{-12}$ m/V)	440
Curie Temperature (°C)	335
Dielectric Constant	1850

Table 5. Distribution of specimen between composite columns

	1 Layer Inserts – 9 mm slices	3 Layer Inserts – 3 mm slices	6 Layer Inserts – 1.5 mm slices	9 Layer Inserts – 1 mm slices
Column 1	2	1	0	0
Column 2	1	1	0	1
Column 3	1	2	1	1
Column 4	1	1	1	1
Column 5	1	1	1	2

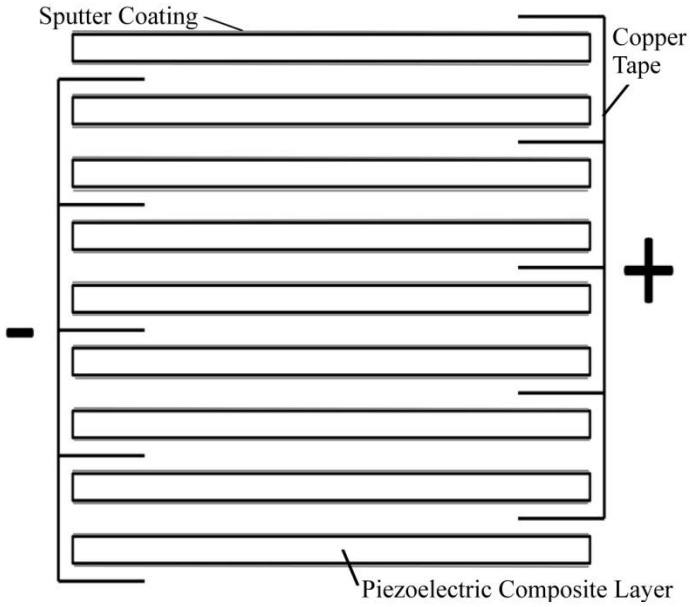

Figure 16. Diagram of electrical connection of a 9 layer specimen

The specimens were poled using an electric field strength of 1 kV/mm for 30 minutes and were then subjected to testing after a 30 minute resting period per lab protocol. Voltages of 1 kV, 1.5 kV, 3 kV, and 9 kV were used to pole the 9 layer, 6 layer, 3 layer, and 1 layer specimens

respectively. Specimens were first tested at 1 force preload, 4 load frequencies, 3 force amplitudes, and 38 load resistances ranging from 420 kΩ to 5 GΩ (Table 6). A force preload level of 1200 N was chosen as a high estimate of the forces seen in the intervertebral space.[32] Loading frequencies of 1, 2, 3, and 5 Hz were chosen based on reasonable estimates of gait frequencies (from walking to running). Force amplitudes of 100, 500, and 1000 N were based on the ranges of force expected to be seen in the intervertebral disc space if a subject has undergone spinal fusion surgery with instrumentation.[32] Load resistances were chosen to give a representative power curve based on the theoretical analysis done in previous work.[32] Testing was performed using a MTS MiniBionix 858 (MTS Corp., Eden Prairie, MN) system with data being recorded at 512 Hz and 15 cycles of data collected for every test parameter. Force was recorded using a 25 kN load cell, axial displacement was recorded using built in capabilities, and voltage output was recorded using built in measurements of the MTS Mini Bionix 858.

Table 6. Test parameters for initial specimen testing

Preload (N)	Load Amplitude (N)	Load Frequency (Hz)
1200	100	1
	100	2
	100	3
	100	5
	500	1
	500	2
	500	3
	500	5
	1000	1
	1000	2
	1000	3
	1000	5

The specimens were tested following the previous test using the same test system, recording the same measurements as the previous test. Specimens were poled using an electric field strength of 2 kV/mm for 15 minutes for 9 layer implants, with the other specimens undergoing the same poling procedure previously used. Voltages of 2 kV, 1.5 kV, 3 kV, and 9 kV were used to pole the 9 layer, 6 layer, 3 layer, and 1 layer inserts respectively.[40] The increased electric field strength was used on the 9 layer specimen to test a new poling technique while providing 1 point of direct comparison. Specimens were tested at 1 force amplitude, 1 load frequency, 6 preload forces, and 4 load resistances (Table 7). The force amplitude of 100 N was chosen as a conservative estimate of forces expected in the intervertebral disc space which would

allow preload levels to be varied as low as 200 N.[32] The load frequency of 2 Hz was chosen as representative of a typical walking frequency (1 Hz for each foot). The preload forces of 200, 400, 600, 800, 1000, and 1200 N were chosen because they are representative of the forces expected in the intervertebral disc space when a subject has undergone spinal fusion surgery with instrumentation. The load resistances of 5.11 kΩ, 9.94 kΩ, and 94.06 kΩ were chosen as resistances similar to the resistance of body tissue (0-40 kΩ) and the resistance of 16.76 MΩ was chosen as a resistance within the range of the previous test to allow direct comparisons.

Table 7. Test parameters for final specimen testing

Load Amplitude (N)	Load Frequency (Hz)	Preload (N)
100	2	200
		400
		600
		800
		1000
		1200

Appendix B. Results and Discussion

Figure 17 shows the results of the comparisons between specimens with different numbers of layers. As the number of layers increased, the optimal load resistance decreased and the power output did not change significantly. Table 8 shows a sample of the p-values obtained using an unequal variance t-test. Eighty percent of the comparisons showed a significantly different power ($p<0.05$).

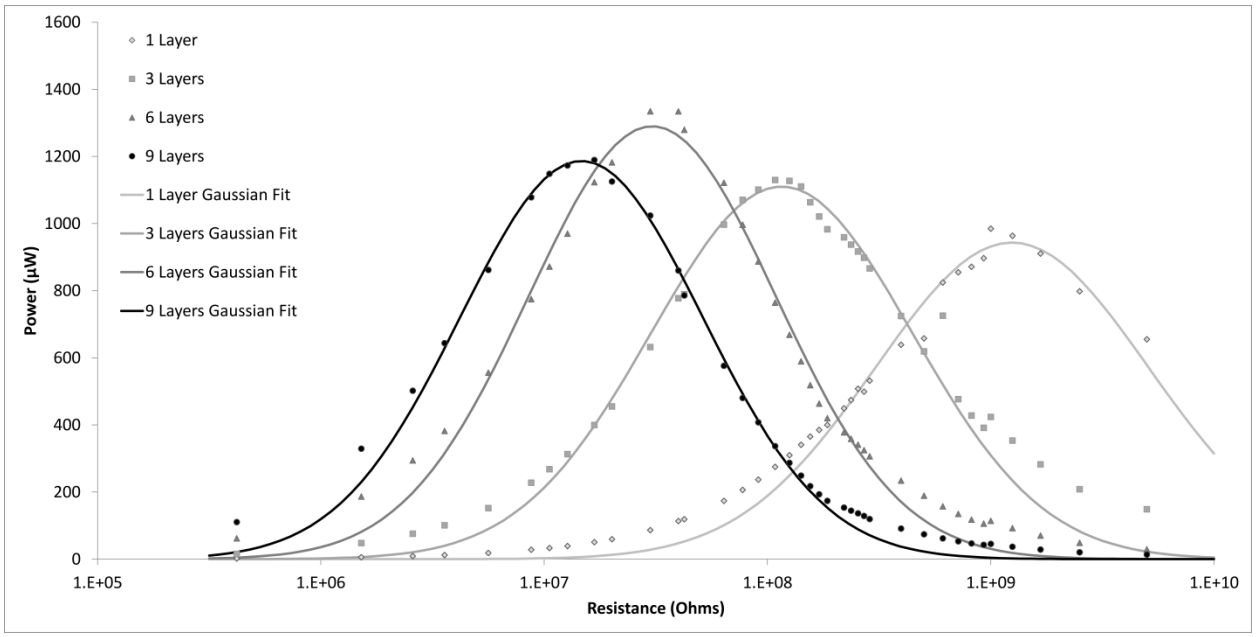

Figure 17. The effects of varying number of layers on power output of specimens at 1000 N and 2 Hz

Table 8. P-values from comparison between specimens with different numbers of layers at 1000N and 2 Hz

Load Resistance	1 v 3 Layer	1 v 6 Layer	1 v 9 Layer	3 v 6 Layer	3 v 9 Layer	6 v 9 Layer
420000	0.000678	0.015315	0.000441	0.023029	0.000619	0.014313
1517000	0.001534	0.021815	0.000545	0.032923	0.000732	0.02427
2579000	0.001759	0.023606	0.000848	0.035744	0.001216	0.034539

3581000	0.002082	0.024154	0.001213	0.036689	0.001807	0.040082
5623000	0.00206	0.023667	0.00151	0.036183	0.002346	0.050753
8750000	0.002162	0.023909	0.001631	0.037058	0.002648	0.072026
10560000	0.002304	0.024025	0.001744	0.03758	0.002909	0.085494
12719000	0.002455	0.02449	0.001881	0.038903	0.003277	0.109768
16777000	0.002399	0.024256	0.002247	0.039443	0.00435	0.17253
20120000	0.002598	0.024731	0.00259	0.04127	0.005524	0.233738
29870000	0.002697	0.02361	0.003806	0.042001	0.01183	0.461168
39910000	0.002604	0.023322	0.003614	0.04553	0.018628	0.352981
42420000	0.002376	0.022779	0.003971	0.045589	0.023889	0.312269
63820000	0.001865	0.021974	0.004979	0.062048	0.165571	0.135328
77420000	0.001986	0.022493	0.005284	0.088599	0.465959	0.095617
91020000	0.001817	0.022845	0.007717	0.135707	0.230219	0.074708
1.08E+08	0.00179	0.023731	0.009413	0.249616	0.05059	0.057083
1.25E+08	0.001768	0.024192	0.010928	0.438133	0.015866	0.050154
1.41E+08	0.002087	0.025209	0.020986	0.373767	0.008571	0.044493
1.55E+08	0.002507	0.027129	0.038574	0.234247	0.006188	0.042205
1.7E+08	0.002726	0.028932	0.07482	0.145377	0.004938	0.041262
1.85E+08	0.00269	0.030499	0.155301	0.094803	0.003845	0.0389
2.2E+08	0.002996	0.034343	0.427759	0.048991	0.003113	0.035288
2.37E+08	0.003053	0.039731	0.408009	0.038453	0.00275	0.035454
2.54E+08	0.003632	0.049543	0.206481	0.030193	0.002631	0.03368
2.71E+08	0.003027	0.050107	0.192727	0.022756	0.002179	0.032261

2.87E+08	0.00331	0.068518	0.098735	0.01776	0.001974	0.031376
3.97E+08	0.006451	0.417424	0.014299	0.00838	0.001693	0.028388
5.03E+08	0.01733	0.209412	0.012749	0.006884	0.001863	0.026596
6.1E+08	0.071596	0.009195	0.000755	0.011471	0.004658	0.025527
7.15E+08	0.224172	0.00295	0.000626	0.004896	0.001705	0.025476
8.2E+08	0.459935	0.001556	0.000561	0.004537	0.00171	0.025454
9.3E+08	0.304846	0.001042	0.000497	0.004756	0.001896	0.024709
1E+09	0.300086	0.000982	0.000469	0.004595	0.001824	0.024557
1.25E+09	0.055482	0.000675	0.000411	0.003794	0.001568	0.022606
1.67E+09	0.007428	0.000537	0.000386	0.003193	0.001442	0.023177
2.5E+09	0.00177	0.000465	0.000371	0.002925	0.001435	0.02348
5E+09	0.000749	0.000362	0.000319	0.003084	0.001809	0.03091

Figure 18 shows the effects of varying the number of layers in the specimens at selected load resistances. The six lowest load resistances (420 kΩ, 1.517 MΩ, 2.579 MΩ, 3.581 MΩ, 5.623 MΩ, and 8.750 MΩ) were selected because the practicality of using such high load resistances with rectifying and regulating circuits. At these load resistances it can be seen that the power output of the inserts increases at every load resistance; the difference was significant in all cases ($p<0.05$).

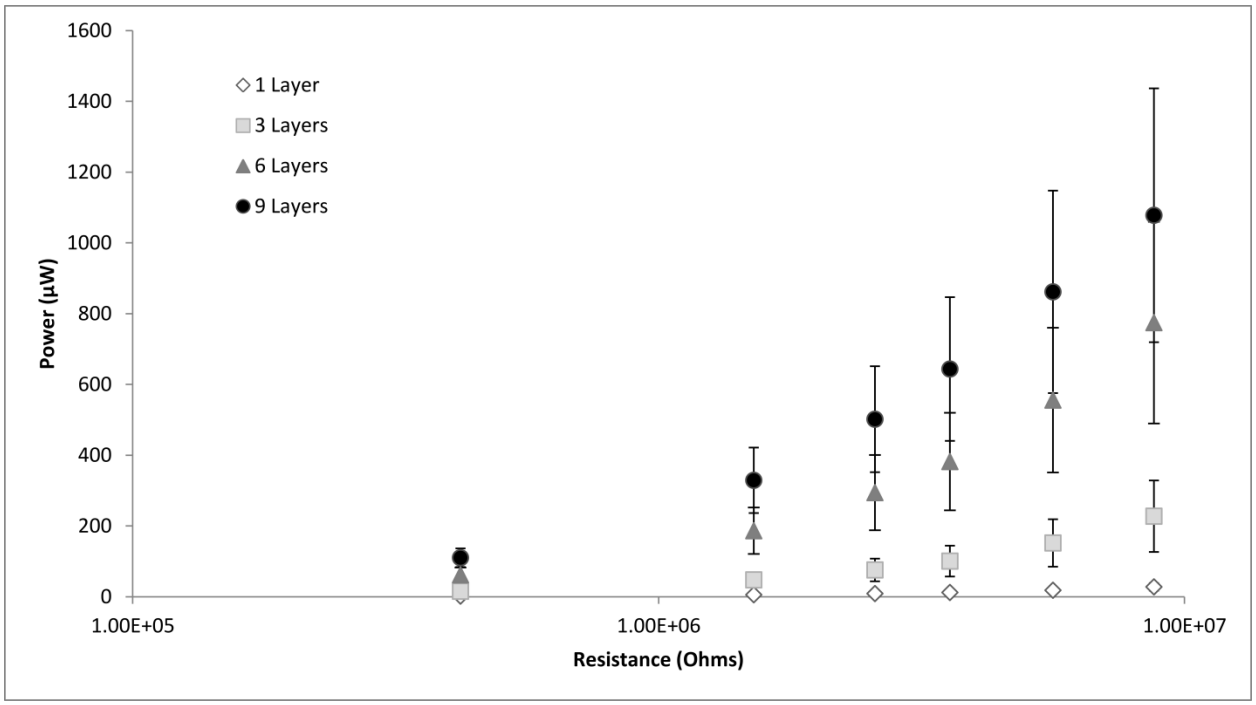

Figure 18. Effects of number of layers on power output of specimens at 1000 N and 2 Hz at selected load resistances

Figure 19 shows the results of comparisons between loading at different frequencies. As the frequency increased, the optimal load resistance decreased and the maximum power output increased. This occurs because piezoelectric materials are essentially capacitive, and thus are highly frequency dependent.[12]

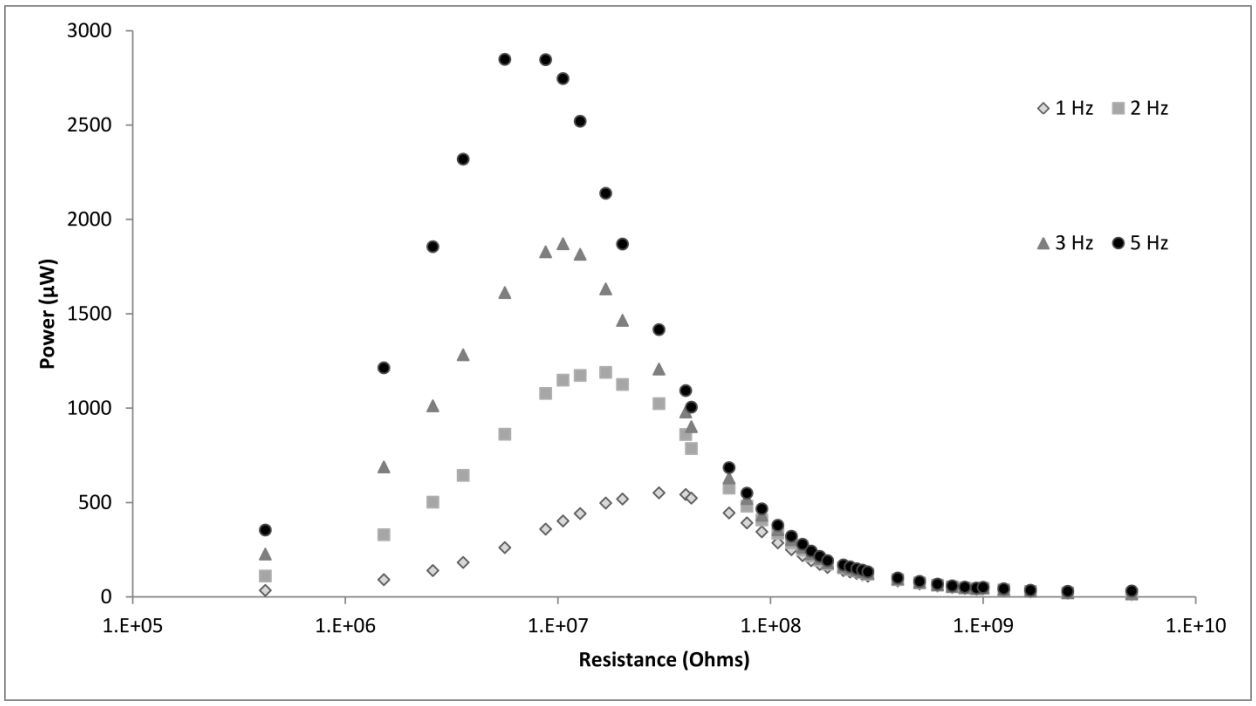

Figure 19. Effects of frequency on power output of 9 layer specimens at 1000 N

Figure 20 shows the effects of preload on the power output of the specimens. The difference between preload levels was statistically insignificant at all tested levels. While studies have shown that preload can affect the resonant frequency of piezoelectic materials[29,30] (and thus the power output at specific frequencies), the loading frequency is so low in this application that preload does not have a significant effect.

Table 9 shows a sample of the p-values obtained using an unequal variance t-test. Over 80% of the comparisons made failed to show a statistically significant difference in comparison ($p<0.05$).

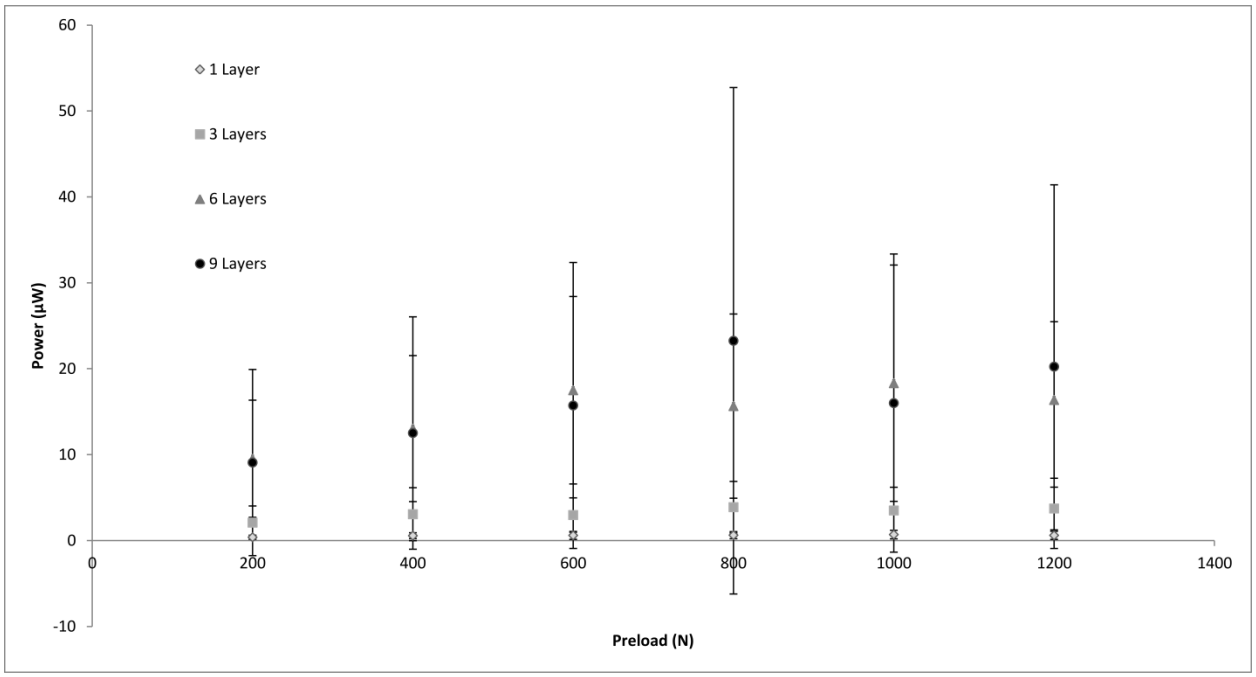

Figure 20. Effects of preload on power output of specimens with 1, 3, 6, and 9 layers at 16.78 MΩ

Table 9. P-values from comparisons between power output of 1 layer specimens at different preloads and 16.78 MΩ

Comparison	P-value
200 N v 400 N	0.0335
200 N v 600 N	0.0655
200 N v 800 N	0.0334
200 N v 1000 N	0.0401
200 N v 1200 N	0.1105
400 N v 600 N	0.3537
400 N v 800 N	0.1807
400 N v 1000 N	0.1108
400 v 1200 N	0.3842
600 N v 800 N	0.2969
600 N v 1000 N	0.1717
600 N v 1200 N	0.4887
800 N v 1000 N	0.1940
800 N v 1200 N	0.3962
1000 N v 1200 N	0.2326

Figure 21 shows the effects of increasing force on power output of the specimens. The power output increases as the force increases, as predicted by equations detailing the basic operation of piezoelectric materials which show that force and electric field strength (and thus power output) are directly related.

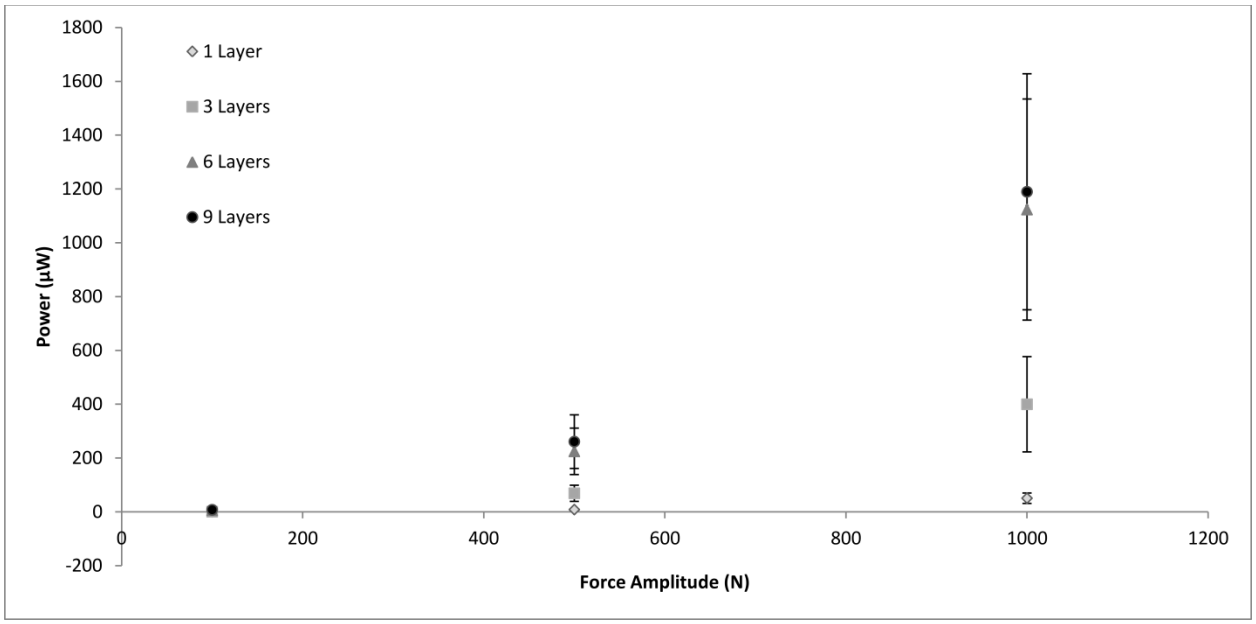

Figure 21. Effects of load amplitude on power output of specimens with 1, 3, 6, and 9 layers at 1000 N, 2 Hz, and 16.78 MΩ

Figure 22 shows the effects of poling procedure on average maximum power output in 9 layer specimens at 2 Hz, 1200 N preload, 100 N load amplitude, and 16.78 MΩ load resistance. Though results were not statistically significant (p=0.10), it can be seen that there is a trend of increased average maximum power output with the increased poling electric field strength.

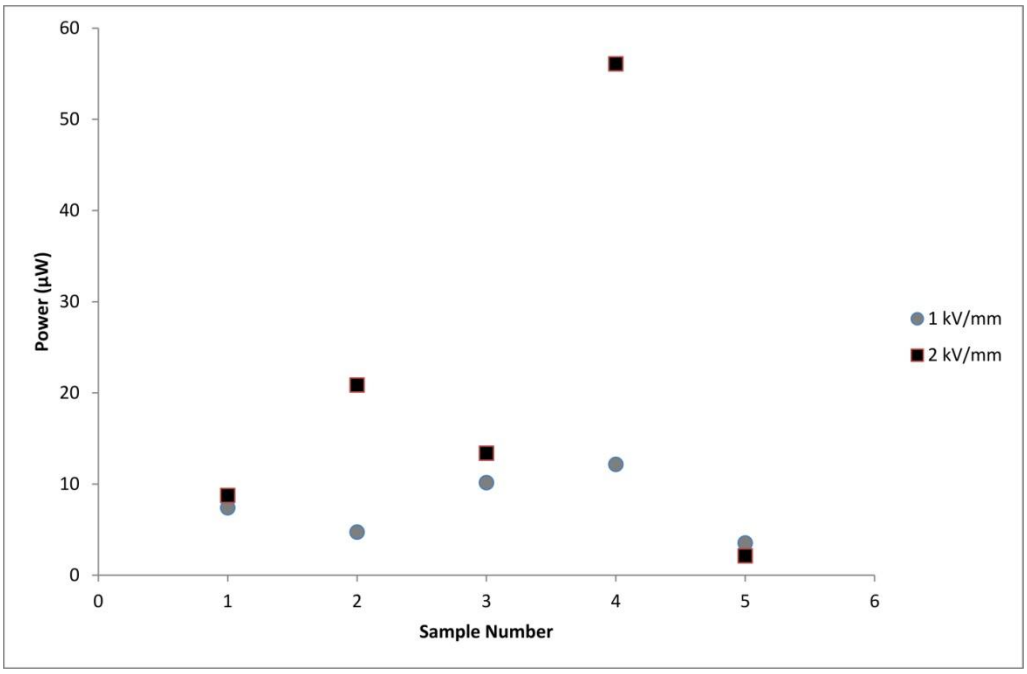

Figure 22. Effects of poling procedure on average maximum power output at 100 N load amplitude, 1200 N preload, 2 Hz, and 16.78 M load resistance